Spectral energy distribution variation in BL Lacs and flat spectrum radio quasars

Bindu Rani,[1,2,3]⋆ Alok C. Gupta,[1,2] R. Bachev,[3] A. Strigachev,[3] E. Semkov,[3]
F. D'Ammando,[4] P. J. Wiita,[5] M. A. Gurwell,[6] E. Ovcharov,[7] B. Mihov,[3] S. Boeva[3]
and S. Peneva[3]

[1]*Aryabhatta Research Institute of Observational Sciences (ARIES), Manora Peak, Nainital 263129, India*
[2]*Department of Physics, DDU Gorakhpur University, Gorakhpur-273009, India*
[3]*Institute of Astronomy and National Astronomical Observatory, Bulgarian Academy of Sciences, 72 Tsarigradsko Shosse Blvd., 1784 Sofia, Bulgaria*
[4]*INAF-IASF Palermo, Via Ugo La Malfa 153, I-90146 Palermo, Italy*
[5]*Department of Physics, The College of New Jersey, PO Box 7718, Ewing, NJ 08628, USA*
[6]*Harvard–Smithsonian Center for Astrophysics, Cambridge, MA 02138, USA*
[7]*Department of Astronomy, University of Sofia, 5 James Bourchier, 1164 Sofia, Bulgaria*

ABSTRACT
We present the results of our study of spectral energy distributions (SEDs) of a sample of 10 low- to intermediate-synchrotron-peaked blazars. We investigate some of the physical parameters most likely responsible for the observed short-term variations in blazars. To do so, we focus on the study of changes in the SEDs of blazars corresponding to changes in their respective optical fluxes. We model the observed spectra of blazars from radio to optical frequencies using a synchrotron model that entails a log-parabolic distribution of electron energies. A significant correlation among the two fitted spectral parameters (a, b) of log-parabolic curves and a negative trend among the peak frequency and spectral curvature parameter, b, emphasize that the SEDs of blazars are fitted well by log-parabolic curves. On considering each model parameter that could be responsible for changes in the observed SEDs of these blazars, we find that changes in the jet Doppler factors are most important.

Key words: radiation mechanisms: non-thermal – galaxies: active – BL Lacertae objects: general.

1 INTRODUCTION

Studies of the two types of blazars, BL Lac objects and flat spectrum radio quasars (FSRQs), have shown that their spectral energy distributions (SEDs) are characterized by a double-peaked luminosity structure (e.g. Ghisellini et al. 1997). The BL Lacs and FSRQs classes are defined according to the absence or presence of strong broad emission lines in their optical/ultraviolet (UV) spectrum, respectively. The low-energy peak is well explained by synchrotron emission from relativistic electrons in a jet closely aligned to the line of sight, with bulk Lorentz factor Γ of order the of 10–100 (e.g. Maraschi, Ghisellini & Celotti 1992; Ghisellini et al. 1993; Hovatta et al. 2009, and references therein). Moreover, the position of the low-energy peak leads to a further classification of the blazars into three categories, depending on the peak frequency of their synchrotron bump, $\nu_{\text{peak}}^{\text{S}}$: low-synchrotron-peaked (LSP) sources, with $\nu_{\text{peak}}^{\text{S}} < 10^{14}$ Hz; intermediate-synchrotron-peaked (ISP) sources, with $10^{14} < \nu_{\text{peak}}^{\text{S}} < 10^{15}$ Hz; and high-synchrotron-peaked (HSP)

sources, with $\nu_{\text{peak}}^{\text{S}} > 10^{15}$ Hz. This scheme is an extension of the classification introduced by Padovani & Giommi (1995) for BL Lacs (see Abdo et al. 2010a, for details).

The high-energy (hard X-ray and γ-ray) component of the SED is usually explained as arising from inverse-Compton (IC) scattering of the same electrons producing the synchrotron emission. These electrons interact either with the synchrotron photons themselves [synchrotron self-Compton (SSC); e.g. Marscher & Gear (1985)] or with external photons originating in the local environment [external Compton (EC)]. In the latter case, soft photons can be produced directly by the accretion disc (e.g. Dermer & Schlickeiser 1993) or indirectly, for instance, those reprocessed by the broad-line region (BLR; e.g. Sikora 1994), or by the dust torus (Błażejowski et al. 2000). Alternative hadronic models, where the γ-rays are produced by high-energy protons, either via proton synchrotron radiation or via secondary emission from photo-pion and photo-pair-production reactions, have also been proposed (see Böttcher et al. 2007, and the references therein for a review).

The shape of these bumps is characterized in the log (νF_ν) versus log ν plot by a smooth spectrum extending through several frequency decades. Below and above the peaks, the spectrum can be

⋆E-mail: bindu@aries.res.in

approximated with simple power-law profiles with spectral indices above and below the peaks (Ghisellini, Maraschi & Dondi 1996), and such power-law spectra are naturally produced if the emitting electrons follow a power-law distribution of energy. Therefore, the broad-band SED of blazars can be well approximated by a simple parabolic function with logarithms of its variables (e.g. Massaro et al. 2004, 2006; Tramacere et al. 2007, and references therein). The log-parabolic function is one of the simplest ways to represent curved spectra and under simple approximations can be obtained via a statistical electron acceleration mechanism where the acceleration probability decreases with the particle energy (Massaro et al. 2006).

The emission from blazars is known to be variable at all wavelengths. The flux variability is often accompanied by spectral changes. These SED changes are very likely associated with changes in the spectra of emitting electrons that arise from differences in the physical parameters of the jet. Hence modelling of blazar broad-band spectra is required to understand the extreme conditions within the emission region. Not only is the broad-band SED crucial to this understanding, but variability information is also needed to allow us to describe how high-emission states arise and how they differ from the low states. This type of study is most important in discriminating between models. Since it is reasonable to assume that only a few parameters of the model will change significantly between different states of the same source, such comparative modelling of broad-band spectra allows us to put rather tight constraints on those model parameters that are likely to change, at least under the assumption that all other parameters are held fixed for the different model fits (e.g. Mukherjee et al. 1999; Petry et al. 2000; Hartman et al. 2001).

In this paper, we focus on the study of changes in the SEDs of BL Lacs and FSRQs corresponding to observed changes in their respective optical fluxes. The SED variations are expected to be produced by changes in the spectra of the emitting electrons which in turn arise from variations in the physical parameters of the emission region. Therefore we needed to first construct models and then investigate how the SEDs observed in different states might be explained through changes in these parameters. More explicitly, we modelled the observed spectra of blazars from radio to optical frequencies using a synchrotron model with the emitting electrons following a log-parabolic distribution of energy. This allows us to try to estimate the factors responsible for short-term optical flares or short-term variability (STV) in blazars. In this paper, we will strictly concentrate on the low-energy hump (synchrotron emission) portion of blazar SEDs. A complete investigation of the entire broad-band SEDs of these objects, including X-ray and γ-ray data, will be performed in the future.

This paper is structured as follows. Section 2 provides a brief description of the multifrequency data we employed. In Section 3, we discuss the SED modelling, and Section 4 provides our results. Our discussion is given in Section 5, and we present our conclusions in Section 6.

2 MULTIFREQUENCY DATA

The multifrequency SED data of our 10 blazars span a frequency range between radio and optical, including mm, submm and infrared (IR) data. These measurements were all taken between 2008 September and 2009 June. Our sample consists of five BL Lacs and five FSRQs, eight of which are LSPs and two of which are ISPs. We selected these sources as they were bright enough for us to obtain day-to-day flux coverage in *B, V, R* and *I* passbands. Certainly,

this number of objects is too small to provide clearly representative samples of the BL Lac and FSRQ classes, and there may be unknown biases in our two groups. Despite the small sample sizes, some general behaviours might be noted in these data and then investigated in more detail in the future with larger samples. The STV in flux as well as in colour of these blazars was recently reported by Rani et al. (2010b). We used this optical data in our SED study and added to them data collected at other frequencies over the same time period. Radio flux densities at 4.5-, 8- and 14.5-GHz frequencies are obtained from the University of Michigan Radio Astronomy Observatory (UMRAO[1]) data base. The mm and submm data are provided by the Submillimeter Array (SMA) Observer Center[2] data base. The near-IR data are collected from the monitoring provided by the Small and Moderate Aperture Research Telescope System (SMARTS[3]).

For investigating the impact of the variations in flux on the source parameters used for modelling the SEDs, we always ascertained two SEDs of the same source that are characterized by a change of at least 0.3 mag in the optical *R* band. The brighter one is denoted as the high state and the fainter as the low state. The time periods during which the different SEDs of all the sources were obtained are listed in the first column of Table 1 immediately below the name of each of the blazars. Details of their optical properties can be found in Rani et al. (2010b). We note that while we tried to obtain and utilize data taken simultaneously, this was rarely possible, and the temporal intervals over which the data needed to produce an SED in a low or high state could be found to range from 3 days through 3 months. Clearly, this lack of simultaneity can lead to substantial uncertainties in the analysis.

3 SED MODELLING

We performed the spectral analysis using a homogeneous synchrotron emission model with log parabola (LP) energy distribution of emitting electrons to fit the lower energy part of observed spectra, i.e. synchrotron spectra. The best-fitting model to each blazar in each of the two states was obtained by a numerical SSC code (Tramacere et al. 2007, 2009). We used an SED code[4] available online.

The simplified model assumes that radiation is produced within a single blob in the jet, which is taken to be moving relativistically at small angle along the line of sight of the observer. Thus the observed radiation has a Doppler boosting factor $\delta = [\Gamma(1 - \beta\cos\theta)]^{-1}$, where β is the velocity of the source divided by the velocity of light, Γ is the Lorentz factor and θ is the angle between the line of sight of observer and direction of motion of the source. The observed SED of blazars has a double-peaked structure, and a simple analytical function that can model the shape of these broad peaks is a parabola in the logarithms of the variables, i.e. a LP. This function has three spectral parameters and can be defined as (Massaro 2006)

$$F(E) = K E^{-[a+b\log(E)]} \text{ keV}, \qquad (1)$$

where *a* is the photon index at an arbitrary energy (usually taken to be 1 keV) and *b* is the measure of spectral curvature of the observed radiation. One advantage of the LP functional form compared to other option is that in LP formulation the curvature around the peak

---

[1] http://www.astro.lsa.umich.edu/obs/radiotel/umrao.php
[2] http://sma1.sma.hawaii.edu/callist/callist.html
[3] http://www.astro.yale.edu/smarts/glast/targets.html
[4] http://tools.asdc.asi.it/

Table 1. Parameters of SED models using LP fits.

Source	$\langle R_{mag} \rangle$	$\log R^a$ (cm)	B^b (G)	δ^c	N^d (cm^{-3})	z^e	$\log \gamma_{min}{}^f$	$\log \gamma_{max}{}^g$	$\log \gamma_0{}^h$	r^i	s^i	$\log \nu F_{\nu Peak}$ (erg cm^{-2} s^{-1})	$\log \nu_{Peak}{}^j$ (Hz)
3C 66A													
2008 October 20–30	14.60	16.8	0.10	15.2	30	0.444	0.2	6	4.00	0.5	3.00	−10.71	14.66
2009 January 20–22	14.05	16.8	0.11	12.2	30	0.444	0.2	6	4.10	0.6	3.00	−10.40	14.80
AO 0235+164													
2008 September	16.00	17.2	0.09	20.0	40	0.94	0.2	6	3.38	1.9	3.65	−10.21	13.07
2008 October 20–30	15.00	17.2	0.09	21.0	40	0.94	0.2	6	3.42	1.9	3.65	−10.07	12.95
2009 January 20–22	17.00	17.2	0.08	18.0	35	0.94	0.2	6	3.34	1.9	3.40	−10.58	13.03
PKS 0420−014													
2008 October 20–30	16.85	17.0	0.60	18.0	35	0.915	0.2	6	2.80	1.1	3.10	−10.81	12.93
2009 January	16.45	17.0	0.60	20.0	37	0.915	0.2	6	2.80	1.1	3.20	−10.69	12.95
S5 0716+714													
2008 October 20–30	15.30	17.0	0.09	14.0	20	0.31	0.2	6	3.60	0.9	3.20	−10.78	13.60
2009 March to May	13.60	17.0	0.085	15.0	15	0.31	0.2	6	4.12	0.75	3.34	−10.29	14.55
PKS 0735+178													
2009 May	15.90	17.13	0.07	12.0	20	0.424	0.2	6	4.00	0.5	3.00	−11.20	14.41
2009 June	15.60	17.13	0.07	12.7	20	0.424	0.2	6	4.00	0.5	3.02	−11.14	14.52
OJ 287													
2008 October 20–30	14.20	17.0	0.10	18.0	20	0.306	0.2	6	3.40	1.5	3.25	−10.07	13.51
2009 March to April	14.70	17.0	0.12	19.0	25	0.306	0.2	6	3.30	1.5	3.45	−10.06	13.21
4C 29.45													
2009 March 20–29	17.00	17.0	0.50	15.0	30	0.729	0.2	6	2.80	1.3	2.95	−10.77	12.96
2009 May	18.20	17.0	0.45	15.0	25	0.729	0.2	6	2.80	1.1	2.95	−11.16	12.91
3C 279													
2009 April	15.40	17.0	0.60	17.0	30	0.5362	0.2	6	2.70	1.7	3.20	−10.20	12.82
2009 June	16.00	17.0	0.65	17.0	30	0.5362	0.2	6	2.70	1.4	3.30	−10.43	12.53
PKS 1510−089													
2009 April	15.40	16.8	0.50	14.0	30	0.36	0.2	6	3.10	1.0	3.155	−10.69	13.41
2009 June	16.00	16.8	0.50	14.0	30	0.36	0.2	6	3.10	0.8	3.155	−11.02	13.45
3C 454.3													
2008 September 4–10	14.70	17.2	0.50	23.0	30	0.859	0.2	6	2.80	2.3	3.35	−9.46	13.22
2008 October 20–30	15.40	17.2	0.48	21.0	30	0.859	0.2	6	2.70	1.9	3.00	−9.81	12.75

[a]Size of emitting region.
[b]Magnetic field.
[c]Doppler boosting factor.
[d]Number density of emitting electrons.
[e]Redshift.
[f]Minimum values of Lorentz factor.
[g]Maximum values of Lorentz factor.
[h]The Lorentz factor corresponding to the energy where s is evaluated.
[i]Spectral parameters of the electron population (see text).
[j]Synchrotron peak frequency in the rest frame of source.

is characterized by a single parameter b, while in other models it is characterized by more complex functions (e.g. Sohn, Klein & Mack 2003; Massaro et al. 2006); however, the limitation is that it is more suited for distributions symmetrically decreasing with respect to peak frequency than is the norm for synchrotron spectra. Although more complex models, such as a power-law plus LP model, should fit the mm and longer wavelengths data better, we do not have good coverage in those bands; further, the simpler LP model has a clear physical motivation, which we now discuss.

Massaro et al. (2004) showed that the log-parabolic spectrum is analytically related to the statistical acceleration mechanism. It is obtained when the acceleration probability, p, depends upon energy itself, i.e.

$$p_i = g/\gamma_i^q \quad (i = 0, 1, 2, ...), \tag{2}$$

where g, and q are positive constants. Such a situation can naturally occur when particles are confined by a magnetic field that has a confinement efficiency that decreases with an increase in the gyration radii of the accelerating particles (Massaro et al. 2006).

The integrated energy distribution of such accelerated particles is given by

$$N(>\gamma) = N(\gamma/\gamma_0)^{-[s-1+r\log(\gamma/\gamma_0)]}, \tag{3}$$

where γ_0 is the minimum Lorentz factor in equation (2), and r and s are the spectral parameters of the electron population and are related to those of the emitted radiation as (Massaro et al. 2006)

$$a = (s-1)/2 \quad \text{and} \quad b = r/4. \tag{4}$$

With these approximations, we can completely specify the SSC model with the following parameters: magnetic field intensity (B), size of emission region (R), Doppler boosting factor (δ), the LP spectral indices (s and r), the number density of emitting electrons (N), the redshift of the source (z) and particle Lorentz factors (γ_{min}, γ_{max} and γ_0). While fitting the SED of blazars using these parameters, we know the value of z, and we hold R, γ_{min} and γ_{max} fixed. It is clear that there is a cut-off in the low-energy part of synchrotron spectra at a frequency around 10^{11} Hz due to synchrotron self-absorption (e.g. Ghisellini et al. 1999; Tavecchio et al. 2002, and references
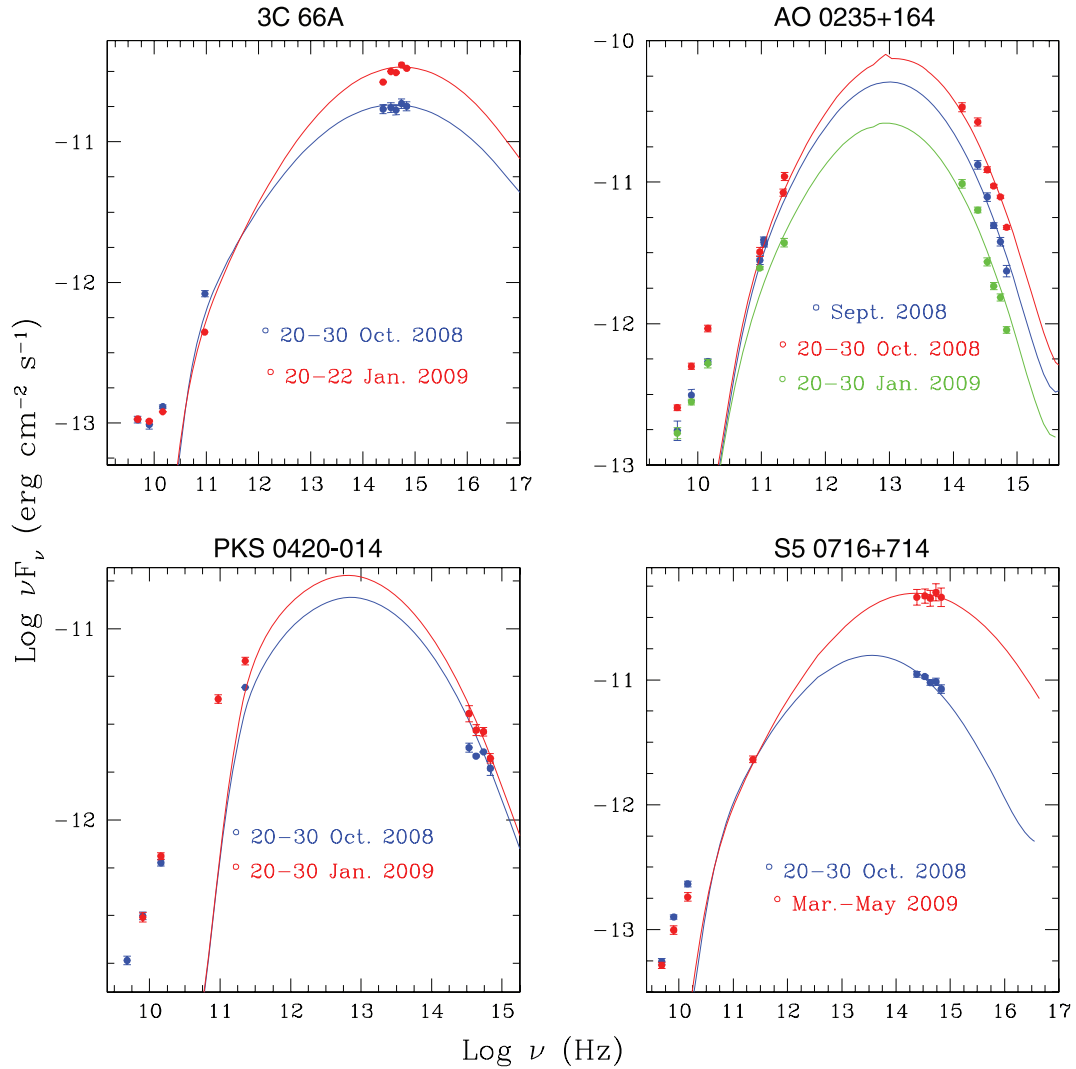
Figure 1. The modelled SED curves of the blazars 3C 66A, AO 0235+164, PKS 0420−014 and S5 0716+714. The points represent the observed data, while best-fitting models are shown by the curves. Since the low-frequency part ($\leq 10^{11}$ Hz) of blazars SEDs is governed by synchrotron-self-absorption mechanism, the modelled SED is steeper below a frequency of 10^{11} Hz (see text for details).

therein), so we consider this self-absorption in modelling the SED of blazars. Because we are looking at STV over the course of a just a few months at most, we feel it justified to assume that R is essentially constant for each source, and we find that the values of γ_{min} and γ_{max} we used for every case give good ranges for the electron energies needed to fit any of the SEDs, and so they are fixed as well. The values of r, s and γ_0 are rather tightly constrained to fit the observed slopes, and we then made over 30 different models for each source to produce the values of all the parameters that yield a 'best fit'.

A direct observation of the synchrotron peak will give a significant help to constrain the model parameters, but, unfortunately, observations of blazars in IR bands, above all in medium and far-IR are not as common as those in the radio, optical and near-IR. Occasionally, this gap can be covered by space-based telescopes such as *Herschel* (Pilbratt et al. 2010). In addition, for FSRQs the SEDs are sometimes overwhelmed by thermal emission from an accretion disc, particularly during low states (Malkan & Sargent 1982), but our code is not able to consider this contribution while modelling the SEDs of blazars. This additional contribution may explain the

excess of optical/UV emission with respect to the best-fitting model for some FSRQs. The values of all these parameters that provide good fits for the two different SEDs of all of the eight LSPs and two ISPs in our sample are listed in Table 1. The fitted SEDs are shown in Figs 1–3.

4 RESULTS

We fit the radio to optical SEDs of 10 blazars with a synchrotron model. The SED curves of all the sources are shown in Figs 1–3, and the fitted parameters are listed in Table 1. Detailed multiband optical STV studies of the fluxes and colours of all of these blazars over the same time period are reported in Rani et al. (2010b). There we showed that the colour versus brightness correlations support the hypothesis that these BL Lacs tend to be bluer with an increase in brightness, while these FSRQs show the opposite trend. Our intraday variability (IDV) study of these sources in the optical R band has been recently reported in Rani et al. (2011). All of these blazars belong to the First Fermi LAT Catalogue (Abdo et al. 2010a), and their spectral properties (hardness, curvature and variability)
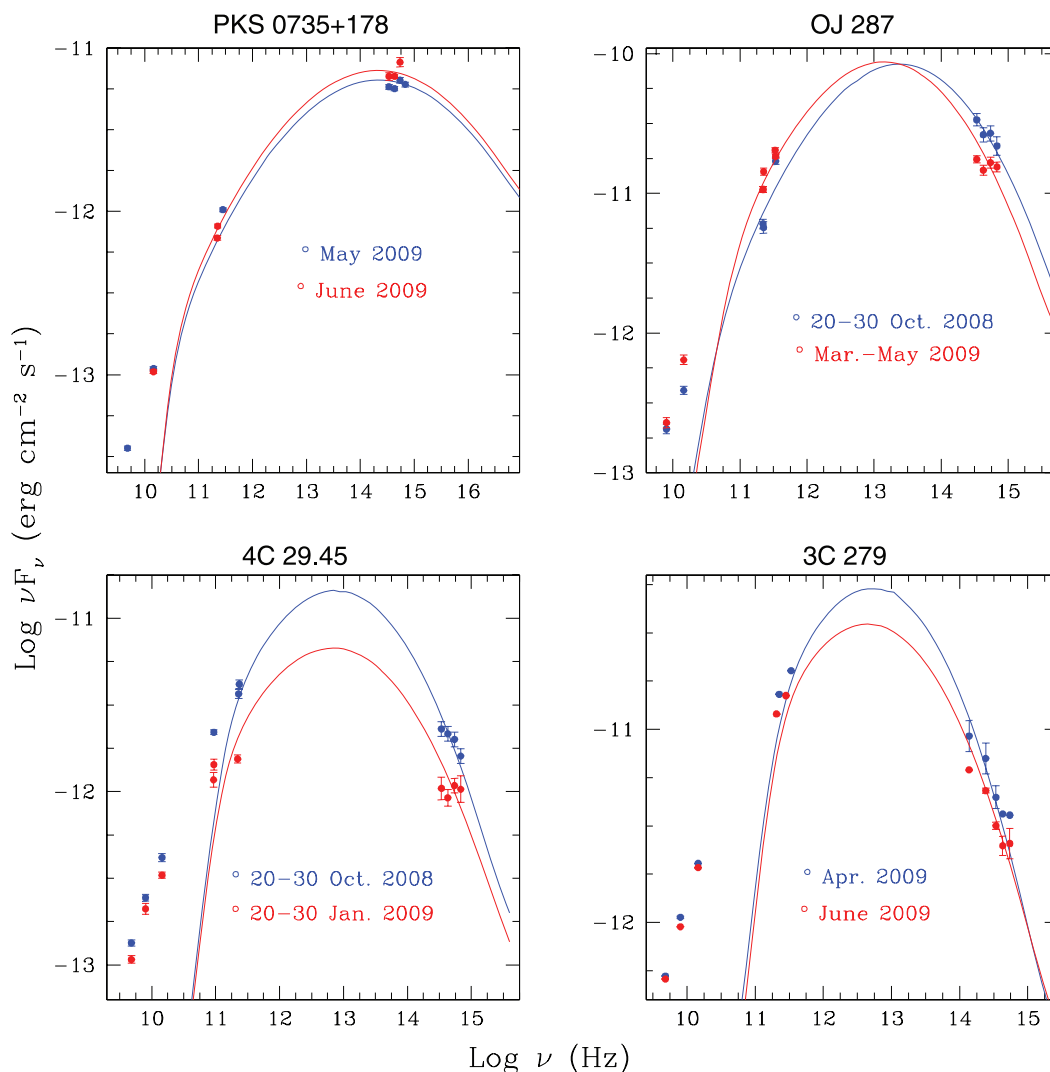
Figure 2. The modelled SED curves of the blazars PKS 0735+178, OJ 287, 4C 29.45 and 3C 279.

at GeV energies have been established by Abdo et al. (2010c). The distribution of photon indices (Γ) above 100 MeV is found to correlate strongly with blazar subclass. Also, the spectral indices tend to be harder when the flux is brighter for both FSRQs and BL Lacs.

We now summarize some previous observations of each of these sources. Since the optical flux, colour and spectral variability of these LSPs and ISPs have already been discussed in Rani et al. (2010b), and IDV studies are in Rani et al. (2011), here we highlight some results from earlier studies of these sources at other wavebands.

3C 66A
This ISP blazar is classified as a BL Lac object. The redshift of 3C 66A was reported as $z = 0.444$ (Miller, French & Hawley 1978), but this value remains uncertain (see Bramel et al. 2005; Yan, Fan & Dai 2010). 3C 66A is observed in radio, IR, optical, X-rays and γ-rays, and shows strong luminosity variations (Teräsranta et al. 2004; Böttcher et al. 2009; Rani et al. 2010b, and references therein). Böttcher et al. (2005) organized an intensive multiwavelength campaign of the source from 2003 July through 2004 April to understand

its broad-band spectral behaviour. Joshi & Böttcher (2007) used a leptonic SSC jet model to reproduce the broad-band SED and the observed optical spectral variability patterns of 3C 66A and made predictions regarding observable X-ray spectral variability patterns and γ-ray emission.

AO 0235+164
The blazar AO 0235+164 at $z = 0.94$ (Nilsson et al. 1996) was classified as a BL Lac object by Spinrad & Smith (1975). An apparent quasi-periodic oscillation of $\sim$17 days has been reported in the X-ray light curves (LCs) of the source by Rani, Wiita & Gupta (2009). The *XMM-Newton* observations suggested the presence of an extra emission component in the source SED in addition to the synchrotron and IC ones. The origin of this component, peaking in the UV/soft X-ray frequency range, is probably thermal emission from an accretion disc, or synchrotron emission from an inner jet region (Raiteri et al. 2006, 2008, and references therein). Hagen-Thorn et al. (2008) reported a significant correlation between the flux density and degree of polarization at optical frequencies and found that at the maximum degree of polarization the electric vector tends to align with the parsec-scale radio jet's direction.
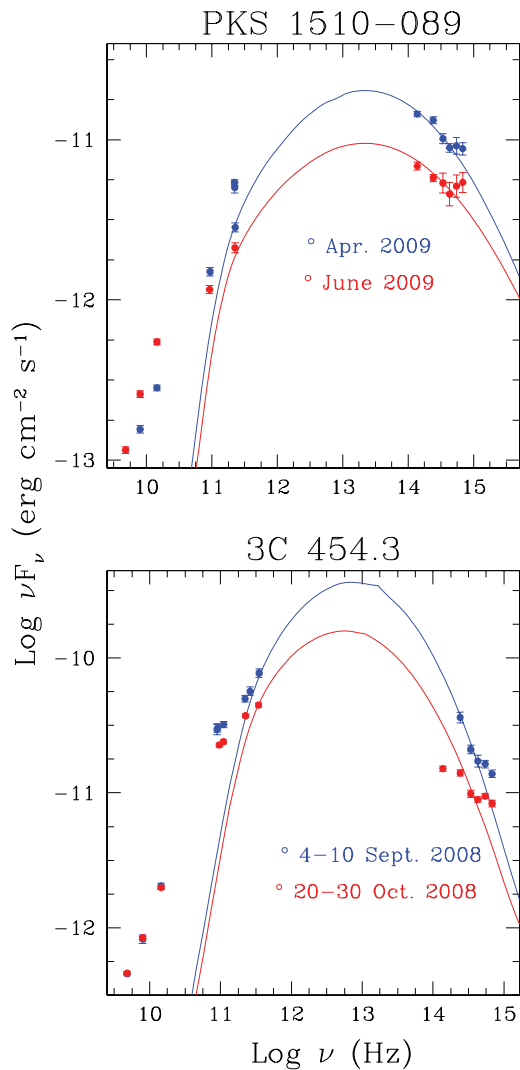
PKS 1510−089

3C 454.3

Figure 3. Modelled SED curves of the blazars PKS 1510−089 and 3C 454.3. The last three points in all of these SEDs are almost certainly dominated by contribution from the disc emission, so we exclude these points while modelling the SEDs of these two FSRQs.

PKS 0420−014

PKS 0420−014 is a FSRQ at a redshift $z = 0.915$ (Kuehr et al. 1981) that has been observed in optical bands since 1969. There is a series of papers reporting the optically active and bright phases of source and semiregular major flaring cycles (e.g. Webb et al. 1988; Villata et al. 1997; Raiteri et al. 1998, and references therein). Rani et al. (2010b) reported that the source tend to be redder with increase in its brightness. Recently, rapid optical and radio brightening of the blazar has been reported by Bach et al. (2010).

S5 0716+714

S5 0716+714 was identified as an ISP (Giommi et al. 1999) at $z = 0.31 \pm 0.08$ (Nilsson et al. 2008). However, Nieppola, Tornikoski & Valtaoja (2006) studied the SED distribution of a large sample of BL Lac objects and categorized 0716+714 as a LSP. Two strong γ-ray flares on 2007 September and October from the source have been detected by *AGILE* (Giommi et al. 2008; Chen et al. 2008). They have also carried out the SED modelling of source with two SSC emission models representative of a slowly and a rapidly variable component, respectively. Villata et al. (2008) reported optical–IR

SED study of the source during the GASP-WEBT-AGILE campaign in 2007. Gupta, Srivastava & Wiita (2009) found high probabilities of quasi-periodic components of ∼25–73 min in the optical LCs observed by Montagni et al. (2006). Recently, nearly periodic oscillations of ∼15 min have been reported in the optical LC of the source by Rani et al. (2010a).

PKS 0735+178

PKS 0735+718 is a highly variable quasar and belongs to the category of BL Lac objects (Carswell et al. 1974). There have been several papers concerning its redshift determination (e.g. Carswell et al. 1974; Falomo & Ulrich 2000, and the references therein) with the most recent result of $z = 0.424$ for PKS 0735+718 found using a *Hubble Space Telescope* (*HST*) snapshot image (Sbarufatti, Treves & Falomo 2005); using that redshift, we classify this source as an ISP. The synchrotron part of the SED of the source peaks at IR–UV, while the low X-ray variability with respect to the high optical–IR variations supports the idea that X-rays are produced by an IC mechanism (Bregman et al. 1984; Madejski & Schwartz 1988). Using 10-year-long multiband optical data of this source, Ciprini et al. (2007) studied the multicolour behaviour, spectral index variations and their correlations with brightness.

OJ 287

OJ 287 (0851+202) ($z = 0.306$) is among the most extensively observed and best studied BL Lac objects with respect to variability. As it is very bright, it is among the very few active galactic nuclei whose optical observations are available for more than a century (Sillanpaa et al. 1996; Gupta et al. 2008). A binary black hole model has been proposed to explain the ∼12 years optical periodicity (Sillanpaa et al. 1996; Valtonen et al. 2008). An intense optical, IR and radio variability study of the source for a time period between 1993 and 1998 has been reported in Pursimo et al. (2000). They detected two major optical outbursts in 1994 November and 1995 December even though the radio flux was very low during the period of outbursts. Using the multiwaveband flux and linear polarization observations and combining with submm polarimetric images, Agudo et al. (2011) argued that the location of the γ-ray emission in prominent flares is >14 pc from the central black hole.

4C 29.45

4C 29.45 ($z = 0.729$; Wills et al. 1983) belongs to the category of FSRQs. Short- and long-term variability at both IR and optical bands has been observed in this source (Noble & Miller 1996; Ghosh et al. 2000). Its optical flux and multicolour variations were studied by Fan et al. (2006). They reported amplitude variations of ∼4.5–6 mag in all passbands (*U, B, V, R, I*) and also suggested that there were possible periods of 3.55 and 1.58 years in the long-term optical LC of the source. The short-term multiband optical colour-brightness studies showed that the source tends to be redder with increase in its brightness (Rani et al. 2010b). Very recently, a GeV flare has been detected in this blazar (Ciprini 2010).

3C 279

3C 279 is both one of the most extensively observed and most violent variable FSRQs across the whole electromagnetic spectrum; it is at a redshift of $z = 0.536$. A comparison of radio to γ-ray SEDs of the source during low and high states of activity in the WEBT campaign of 2006 is presented in Böttcher et al. (2007). Collmar et al. (2010) carried out a multifrequency variability study of the source during 2006 January. A complete compilation of all simultaneous SEDs of 3C 279 collected during the lifetime of Compton Gamma Ray Observatory (CGRO), including modelling of those

SEDs with a leptonic jet model, is presented in Hartman et al. (2001). Recently, Abdo et al. (2010b) report the coincidence of a γ-ray flare with a dramatic change of optical polarization angle. This provides evidence for co-spatial optical and γ-ray emission regions and indicates a highly ordered jet magnetic field.

PKS 1510−089

PKS 1510−089 is classified as a FSRQ at a redshift of $z = 0.361$ (Thompson, Djorgovski & de Carvalho 1990). It also belongs to the category of highly polarized quasars and was detected in the MeV–GeV energy band by the EGRET instrument onboard the CGRO (Hartman et al. 1992). The IC component is dominated by the γ-ray emission, and the synchrotron emission peaked around IR frequencies, even if there is clearly visible in this source a pronounced UV bump, possibly caused by the thermal emission from the accretion disc (Malkan & Moore 1986; Pian & Treves 1993). The multiwavelength flux and SED variability study of the source during its high γ-ray activity period between 2008 September and 2009 June has been reported by Abdo et al. (2010b). Recently, D'Ammando et al. (2011) reported the detailed analysis of multifrequency coverage of extreme γ-ray activity from the source observed by *AGILE* in 2009 March. They have also carried out broad-band SED study of the source and found thermal features in the optical/UV spectrum of the source during the high γ-ray state.

3C 454.3

3C 454.3 is a FSRQ at a redshift of $z = 0.859$ and is one of the most intense and variable of these sources (Pian et al. 2006; Villata et al. 2007; Gupta et al. 2008, and references therein). It is the brightest and most variable blazar at GeV energies (e.g. Raiteri et al. 2008; Vercellone et al. 2008, 2010). The multiflare variability and SED study of the source in 2007 December and 2009 December is reported by Donnarumma et al. (2009) and Pacciani et al. (2010), respectively. The flaring behaviour of the source across the whole electromagnetic spectrum is studied by Jorstad et al. (2010). They conclude that the emergence of a superluminal knot from the core yields a series of optical and high-energy outbursts, and that the millimetre-wave core lies at the end of the jets' acceleration and collimation zone.

5 DISCUSSION

5.1 Statistical particle acceleration and log-parabolic spectra

Massaro et al. (2004) showed that when the acceleration efficiency is inversely proportional to the accelerating particle's energy itself, the energy distribution function, i.e. spectrum, approaches a log-parabolic shape. Therefore, the log-parabolic spectra are naturally produced when the probability of statistical acceleration is energy-dependent. According to this model, the curvature of emitting electron population (r) is related to fractional acceleration gain (ϵ) as $r \propto 1/\epsilon$. Also, $E_P \propto \epsilon$ follows a negative trend between E_P and b (see Tramacere et al. 2009), where E_P is the peak energy of observed SEDs.

Therefore, if the above analysis is correct, then one should expect a negative trend between E_P or ν_P and b, where ν_P is the peak frequency of observed SEDs. We analysed the correlation between the two quantities using our data and found a significant negative correlation between ν_P and b, with $r_P = -0.74$ and p-value = 0.000 14, where r_P is the linear Pearson correlation coefficient and the p-value for the null hypothesis of no correlation corresponds to a significance level >99.98 per cent (Fig. 4). Therefore, our result confirms that the spectral curvature parameter decreases as E_P
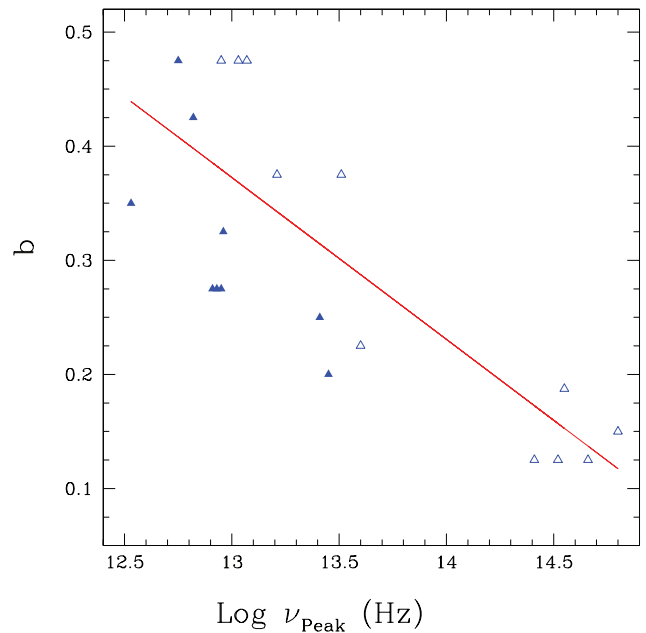
Figure 4. Curvature (b) versus peak frequency (ν_P). A clear relation can be seen between the two quantities which is confirmed by a correlation analysis. The open symbols in this and subsequent figures represent BL Lacs, while the filled symbols stand for FSRQs. The straight line is the best linear fit with a slope $m = -0.14$ and a constant $c = 2.22$ ($y = mx + c$).

moves towards higher energies and means that the blazars' spectra in our cases are fitted well by the log-parabolic model.

On the other hand, such a connection of log-parabolic spectra with acceleration may also be understood in the framework provided by the Fokker–Planck equation with momentum diffusion term (Kardashev, Kuz'min & Syrovatskii 1962; Massaro et al. 2006; Tramacere et al. 2009). They showed that the log-parabolic spectrum results from a Fokker–Planck equation with a momentum diffusion term and a mono-energetic or quasi-mono-energetic injection where the diffusion term acts to broaden the shape of the peak of the distribution. Kardashev et al. (1962) showed that the curvature term, $r \propto 1/(Dt)$, where D is the Diffusion term. This relation leads to the following trend (Tramacere et al. 2009):

$$\ln(E_P) = 2\ln(\gamma_P) + \frac{3}{5b}. \tag{5}$$

Therefore, both the momentum-diffusion term, D, and the fractional acceleration gain term, ϵ, can explain the anticorrelation between E_P and b.

An interesting check if the log-parabolic curve is actually related to the statistical acceleration is the existence of a linear relation between the two spectral parameters a and b (Massaro et al. 2004). Therefore, we checked the correlation among these two quantities and found that they are significantly correlated, with $r_P = 0.61$ and p-value = 0.003 (see Fig. 5). Therefore, we consider that in our case the LP-type spectra are very likely to be characterized by a full statistical acceleration mechanism working on the emitting electrons.

5.2 The cause of blazar SED changes

There are several possibilities that could be invoked to explain the changes in the synchrotron spectra. In the following subsections, we will discuss some of them in detail.
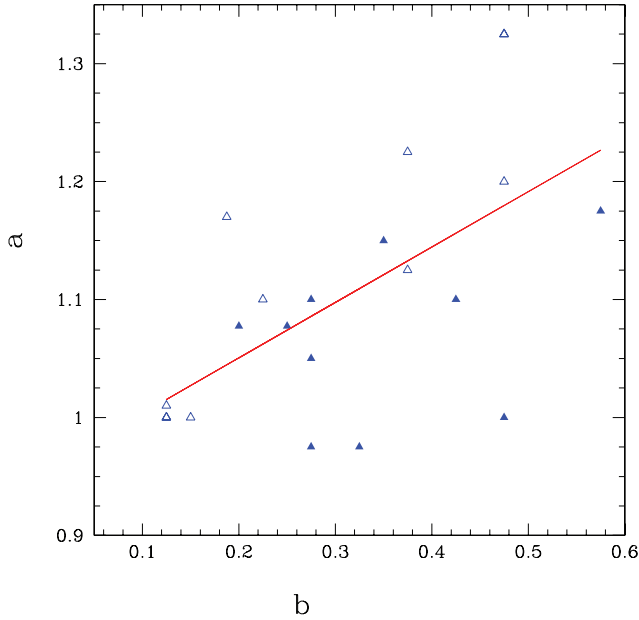
Figure 5. The spectral parameters, *a* and *b*. A clear relation can be seen between the two quantities which is confirmed by a correlation analysis. The straight line is the best linear fit with $m = 0.47$ and $c = 0.96$.

Figure 6. Changes in the peak intensity versus change in peak frequency for all blazars (both BL Lacs and FSRQs together). There is no significant correlation found between the two quantities.

5.2.1 Evolution of the particle energy density distribution

The energy loss of the emitting particles is known to follow $d\gamma/dt \cong -C\gamma^2$, where γ is the Lorentz factor and C is a constant for both the synchrotron and IC emission (Rybicki & Lightman 1979). The evolution of the relativistic particles can be described by energy-dependent Fokker–Planck equation (see for instance Kembhavi & Narlikar 1999):

$$\frac{\partial(\gamma, t)}{\partial t} = -\frac{\partial}{\partial \gamma}\left(\frac{d\gamma}{dt}n(\gamma, t)\right) + Q(\gamma, t), \qquad (6)$$

where $n(\gamma, t)$ is the electron density distribution (a function of energy and time) and $Q(\gamma, t)$ is the time-dependent injection rate. The solutions to the equation above are typically rather complex and can be obtained in terms of Green's functions for the general case.

If the changes in the blazar SEDs are due to a gradual change of the electron energy density distribution due to the synchrotron and IC losses, with no other injections meanwhile, then one should see both a total synchrotron energy decrease and mostly a decrease in γ_b of the electron energy distribution (and therefore the frequency of the synchrotron emission peak). On the other hand, freshly injected electrons between the observational epochs (their energy should be higher than the average as it is expected to decrease in time) should reflect in the opposite behaviour (higher synchrotron emission and a peak blueshift). Therefore, in general one should expect to see a relation between the peak intensity and the peak frequency changes. To search for such a relation, we used correlation analysis statistics (see Fig. 6). The correlation statistics revealed that there is no significant correlation between the two quantities as $r_P = 0.48$ corresponding to a p-value $= 0.084$, where r_P is the linear Pearson correlation coefficient and p is a null hypothesis probability value. As there is no significant relation found between the two quantities, perhaps electron energy density evolution/electron injection is not the primary driver of the SED changes.
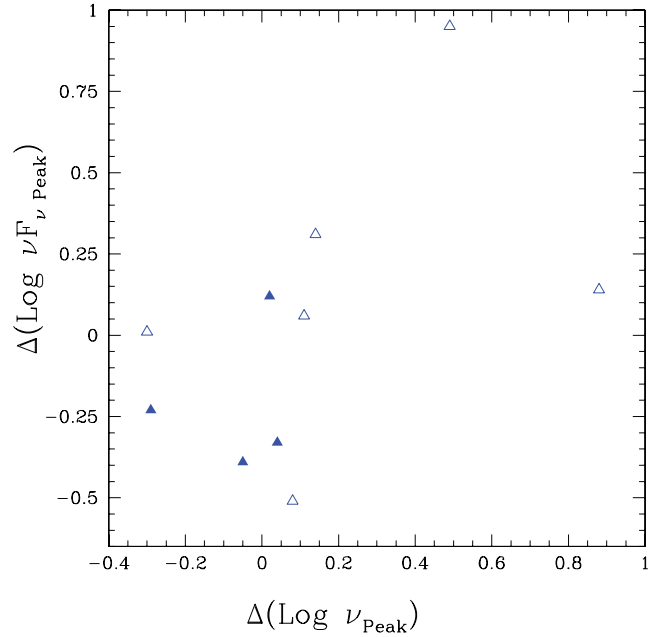
5.2.2 Change of the Doppler boosting factor

Another effect that can modify the blazar synchrotron emission is the change of the Doppler boosting factor, presumably due to a change in either the bulk velocity or the viewing angle. Raiteri et al. (2010) also found that only geometrical (Doppler factor) changes are capable of explaining SED variations between two epochs for BL Lac. The changes of the synchrotron peak intensity versus Doppler factor variations for our sample of blazars are shown in Fig. 7. We can see a clear relation among the two quantities, and it is confirmed by values of $r_P = 0.51$ and p-value $= 0.05$. We also searched for a correlation between change in R-band magnitude versus change in respective Doppler factor values. This would be relevant if $\langle R \rangle$ is a somewhat more representative quantity for the synchrotron emission rather than peak intensity. Again, we found significant correlation among ΔR_{mag} and $\Delta \delta$ (see Fig. 8). Therefore, we consider that Doppler factor changes are a strong driver that can be responsible for the SED changes.

5.2.3 Change of the magnetic field

Since the value of the magnetic field, B, is related to the location of the dissipation region, if the two SEDs arise from periods of different activity, it is quite possible that the emission was produced by blobs that dissipate at different locations in the jet. In that case, we expect to find different B values for the different SEDs of our sources. The change in B values can also lead to variations in the flux of these sources, which will be reflected in the two different SEDs of the sources. Therefore, we search for a correlation between the change in $\langle R \rangle$ and that in B (Fig. 9), but we do not find any significant correlation among them for all of our blazars. However, we note an apparent significant correlation among these two parameters for the BL Lacs alone, which is confirmed by a correlation analysis ($r_P = 0.96$, $p = 0.002$ for BL Lacs). Therefore, we conclude that changes in magnetic field strength may be responsible for the SED changes in the case of BL Lacs.
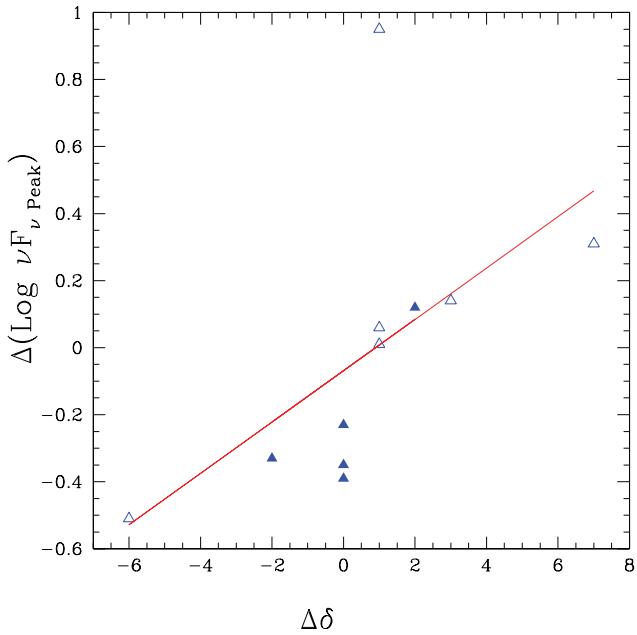
Figure 7. Changes in the peak intensity versus change in Doppler factor for all blazars that have multiple SEDs in our sample. There is a clear relation seen between the two quantities. The straight line is the best linear fit with $m = 0.07$ and $c = -0.07$.
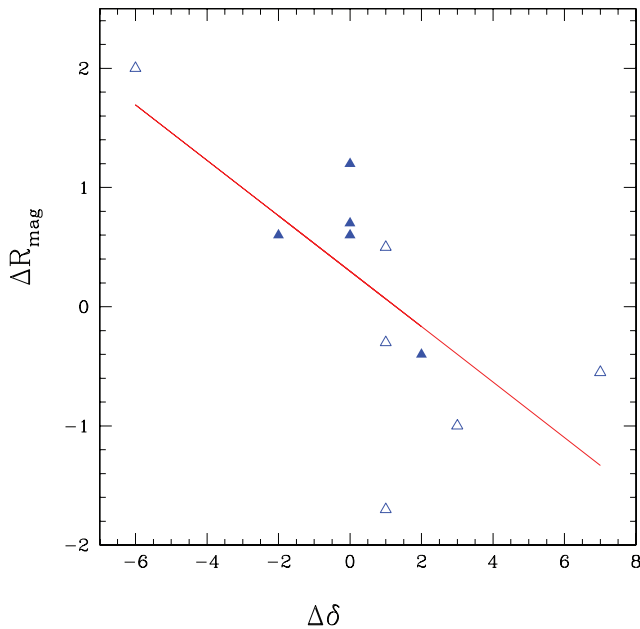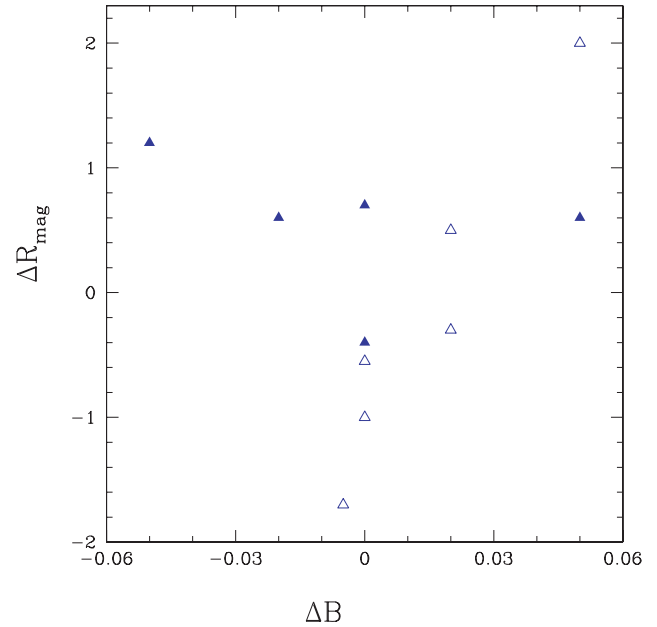

Figure 8. Changes in the R-band magnitude versus change in Doppler factor for all blazars that have multiple SEDs in our sample. There is a significant correlation between the two quantities, with $r_P = -0.70$ and p-value $= 0.01$. The straight line is the best linear fit with $m = -0.23$ and $c = 0.29$.

6 CONCLUSIONS

We have carried out the radio to optical through mm, submm and IR SED studies of a sample of 10 blazars including five BL Lacs and five FSRQs, eight of which are LSPs, while the other two are ISPs. We modelled the SEDs of blazars using synchrotron spectra with log-parabolic distributions. We found a significant negative correlation among ν_{Peak} and the curvature term, r, which implies that the acceleration efficiency of emitting electrons is inversely

Figure 9. Changes in the R-band magnitude versus change in magnetic field for all blazars that have multiple SEDs in our sample. There is no significant correlation between the two quantities with $r_P = 0.11$ and p-value $= 0.75$.

proportional to energy itself; however, this correlation can also be explained by the momentum diffusion term in the solution of Fokker–Planck equation. Also, a significant correlation between the two spectral parameters, a and b, implies that the log-parabolic curve is likely to be related to the statistical acceleration of emitting electrons.

Of course, our modelling has significant limitations. We are assuming that only one zone dominates the emission at any given time, and this is unlikely to be an excellent approximation. Although we strived for data obtained simultaneously, this was often impossible to obtain; therefore, any variations within the 'high' and 'low' states have been averaged over time bins ranging from days to 2 months. This lack of simultaneity could have vitiated our results but only appears to have added scatter to all of Figs 4–9.

We considered each likely factor that could be responsible for the changes in observed SEDs of blazars. If the electron energy density evolution governs the SED changes, then one should expect a correlation between change in peak intensity versus change in peak frequency. Since we do not observe any such correlation, we consider that the evolution of electron energy density probably is not responsible for the observed SED changes. Also, for our entire sample of blazars, changes in $\langle R_{mag} \rangle$ are not correlated with the respective changes in B, so the change in magnetic field strength is probably not responsible for the SED changes we saw. However, for the BL Lacs alone, the SED changes may be driven by changes in B. We find that the change in Doppler factor is significantly correlated with the change in peak intensity as well as with $\langle R_{mag} \rangle$. Therefore, it is reasonable to suggest that the change in Doppler factor (either bulk velocity or viewing angle) is the primary driver that governs the SED changes in STV in blazars.

REFERENCES

Abdo A. A. et al., 2010a, ApJ, 716, 30
Abdo A. A. et al., 2010b, ApJ, 721, 1425
Abdo A. A. et al., 2010c, ApJS, 188, 405
Agudo I. et al., 2011, ApJ, 726, L13
Bach U., Fuhrmann L., Konstantinova T., Larionov V. M., Raiteri C. M., Villata M., Leto P., 2010, Astron. Telegram, 2395, 1
Błażejowski M., Sikora M., Moderski R., Madejski G. M., 2000, ApJ, 545, 107
Böttcher M. et al., 2005, ApJ, 631, 169
Böttcher M. et al., 2007, ApJ, 670, 968
Böttcher M. et al., 2009, ApJ, 694, 174
Bramel D. A. et al., 2005, ApJ, 629, 108
Bregman J. N. et al., 1984, ApJ, 276, 454
Carswell R. F., Strittmatter P. A., Williams R. E., Kinman T. D., Serkowski K., 1974, ApJ, 190, L101
Chen A. W. et al., 2008, A&A, 489, L37
Ciprini S., 2010, Astron. Telegram, 2795, 1
Ciprini S. et al., 2007, A&A, 467, 465
Collmar W. et al., 2010, A&A, 522, A66
D'Ammando F. et al., 2011, A&A, 529, A145
Dermer C. D., Schlickeiser R., 1993, ApJ, 416, 458
Donnarumma I. et al., 2009, ApJ, 707, 1115
Falomo R., Ulrich M., 2000, A&A, 357, 91
Fan J. et al., 2006, PASJ, 58, 945
Ghisellini G., Padovani P., Celotti A., Maraschi L., 1993, ApJ, 407, 65
Ghisellini G., Maraschi L., Dondi L., 1996, A&AS, 120, C503
Ghisellini G. et al., 1997, A&A, 327, 61
Ghisellini G. et al., 1999, A&A, 348, 63
Ghosh K. K., Ramsey B. D., Sadun A. C., Soundararajaperumal S., 2000, ApJS, 127, 11
Giommi P. et al., 1999, A&A, 351, 59
Giommi P. et al., 2008, A&A, 487, L49
Gupta A. C., Fan J. H., Bai J. M., Wagner S. J., 2008, AJ, 135, 1384
Gupta A. C., Srivastava A. K., Wiita P. J., 2009, ApJ, 690, 216
Hagen-Thorn V. A., Larionov V. M., Jorstad S. G., Arkharov A. A., Hagen-Thorn E. I., Efimova N. V., Larionova L. V., Marscher A. P., 2008, ApJ, 672, 40
Hartman R. C. et al., 1992, ApJ, 385, L1
Hartman R. C. et al., 2001, ApJ, 553, 683
Hovatta T., Valtaoja E., Tornikoski M., Lähteenmäki A., 2009, A&A, 494, 527

Jorstad S. G. et al., 2010, ApJ, 715, 362
Joshi M., Böttcher M., 2007, ApJ, 662, 884
Kardashev N. S., Kuz'min A. D., Syrovatskii S. I., 1962, SvA, 6, 167
Kembhavi A. K., Narlikar J. V., 1999, in Kembhavi A. K., Narlikar J. V., eds, Quasars and Active Galactic Nuclei. Cambridge Univ. Press, Cambridge
Kuehr H., Witzel A., Pauliny-Toth I. I. K., Nauber U., 1981, A&AS, 45, 367
Madejski G. M., Schwartz D. A., 1988, ApJ, 330, 776
Malkan M. A., Moore R. L., 1986, ApJ, 300, 216
Malkan M. A., Sargent W. L. W., 1982, ApJ, 254, 22
Maraschi L., Ghisellini G., Celotti A., 1992, ApJ, 397, L5
Marscher A. P., Gear W. K., 1985, ApJ, 298, 114
Massaro E., Perri M., Giommi P., Nesci R., 2004, A&A, 413, 489
Massaro E., Tramacere A., Perri M., Giommi P., Tosti G., 2006, A&A, 448, 861
Miller J. S., French H. B., Hawley S. A., 1978, ApJ, 219, L85
Montagni F., Maselli A., Massaro E., Nesci R., Sclavi S., Maesano M., 2006, A&A, 451, 435
Mukherjee R. et al., 1999, ApJ, 527, 132
Nieppola E., Tomikoski M., Valtaoja E., 2006, A&A, 445, 441
Nilsson K., Charles P. A., Pursimo T., Takalo L. O., Sillanpaeae A., Teerikorpi P., 1996, A&A, 314, 754
Nilsson K., Pursimo T., Sillanpää A., Takalo L. O., Lindfors E., 2008, A&A, 487, L29
Noble J. C., Miller H. R., 1996, in Miller H. R., Webb J. R., Noble J. C., eds, ASP Conf. Ser. Vol. 110, Blazar Continuum Variability. Astron. Soc. Pac., San Francisco, p. 30
Pacciani L. et al., 2010, ApJ, 716, L170
Padovani P., Giommi P., 1995, MNRAS, 277, 1477
Petry D. et al., 2000, ApJ, 536, 742
Pian E., Treves A., 1993, ApJ, 416, 130
Pian E. et al., 2006, A&A, 449, L21
Pilbratt G. L. et al., 2010, A&A, 518, L1
Pursimo T. et al., 2000, A&AS, 146, 141
Raiteri C. M., Ghisellini G., Villata M., de Francesco G., Lanteri L., Chiaberge M., Peila A., Antico G., 1998, A&AS, 127, 445
Raiteri C. M. et al., 2006, A&A, 459, 731
Raiteri C. M. et al., 2008, A&A, 480, 339
Raiteri C. M. et al., 2010, A&A, 524, A43
Rani B., Wiita P. J., Gupta A. C., 2009, ApJ, 696, 2170
Rani B., Gupta A. C., Joshi U. C., Ganesh S., Wiita P. J., 2010a, ApJ, 719, L153
Rani B. et al., 2010b, MNRAS, 404, 1992
Rani B., Gupta A. C., Joshi U. C., Ganesh S., Wiita P. J., 2011, MNRAS, 413, 2157
Rybicki G. B., Lightman A. P., 1979, Radiative Processes in Astrophysics. Wiley, New York
Sbarufatti B., Treves A., Falomo R., 2005, ApJ, 635, 173
Sikora M., 1994, ApJS, 90, 923
Sillanpaa A. et al., 1996, A&A, 305, L17
Sohn B. W., Klein U., Mack K., 2003, A&A, 404, 133
Tavecchio F. et al., 2002, ApJ, 575, 137
Teräsranta H. et al., 2004, A&A, 427, 769
Thompson D. J., Djorgovski S., de Carvalho R., 1990, PASP, 102, 1235
Tramacere A. et al., 2007, A&A, 467, 501
Tramacere A., Giommi P., Perri M., Verrecchia F., Tosti G., 2009, A&A, 501, 879
Valtonen M. J. et al., 2008, Nat, 452, 851
Vercellone S. et al., 2008, ApJ, 676, L13
Vercellone S. et al., 2010, ApJ, 712, 405
Villata M. et al., 1997, A&AS, 121, 119
Villata M. et al., 2007, A&A, 464, L5
Villata M. et al., 2008, A&A, 481, L79
Webb J. R., Smith A. G., Leacock R. J., Fitzgibbons G. L., Gombola P. P., Shepherd D. W., 1988, AJ, 95, 374
Wills B. J. et al., 1983, ApJ, 274, 62
Yan D., Fan Z., Dai B., 2010, preprint (arXiv:1011.1537)

This paper has been typeset from a TEX/LATEX file prepared by the author.